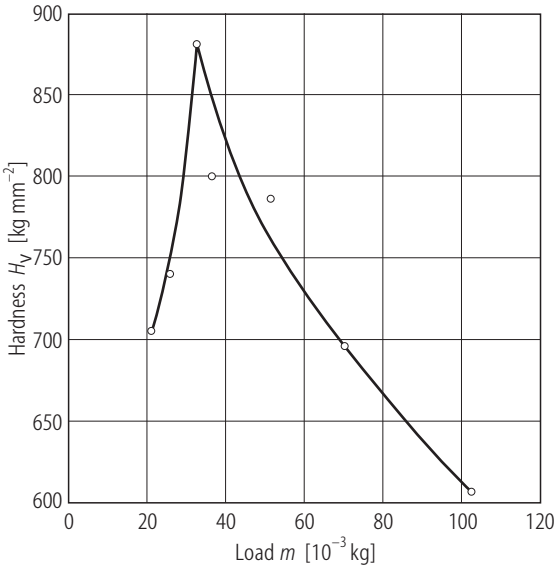

Fig. 2A-1-001. $LiNbO_3$. H_V vs. load m [94Dha]. H_V: Vickers hardness number. Measurement was done on the *c*-faces.

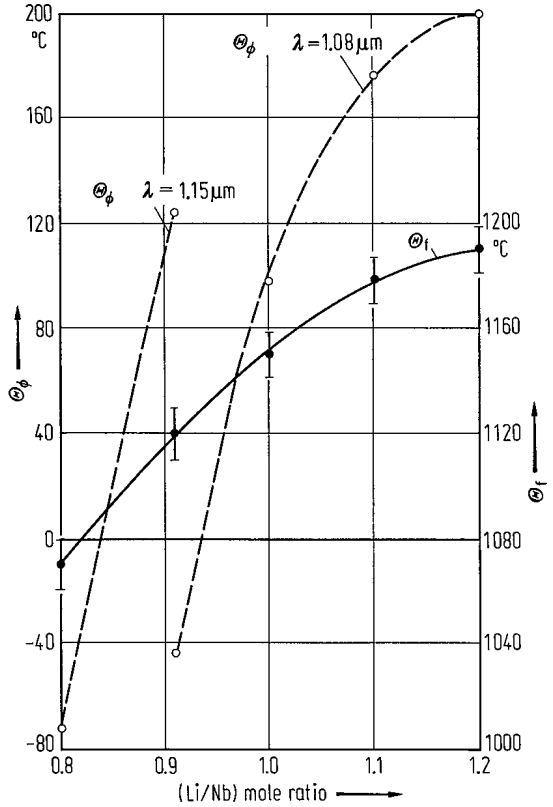

Fig. 2A-1-002. $LiNbO_3$. Θ_f, Θ_ϕ vs. melt composition [68Ber2]. Θ_ϕ: phase matching temperature in optical second harmonic generation. Θ_f and Θ_ϕ are those for grown crystals.

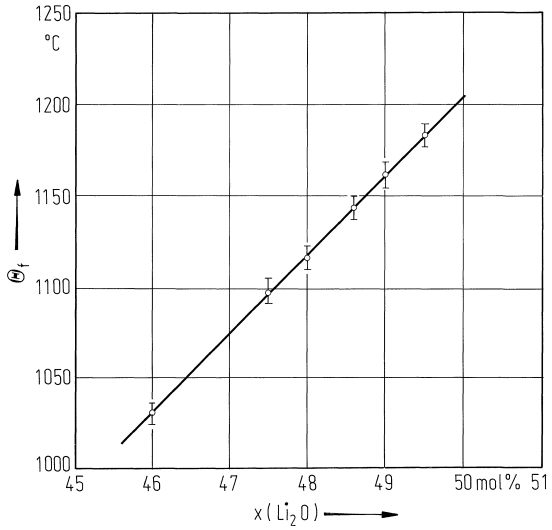

Fig. 2A-1-003. x Li_2O·(1–x)Nb_2O_5. Θ_f vs. x [81Gue].

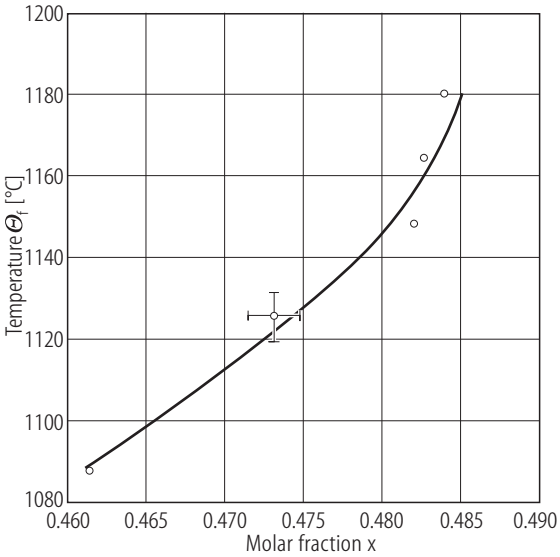

Fig. 2A-1-004. x $Li_2O·(1–x)Nb_2O_5$. Θ_f vs. x [91Gra]. x: Li_2O content.

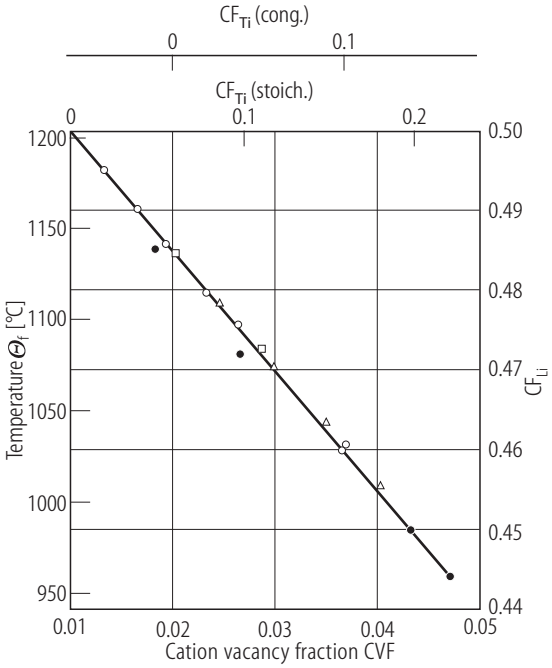

Fig. 2A-1-005. $LiNbO_3$. Θ_f vs. CVF [88Gal]. CVF: cation vacancy fraction. CF_{Ti}: Ti fraction content. CF_{Li}: Li fraction content. Open circles: no TiO_2. Squares: Li / (Li + Nb) = 0.4845. Triangles: Li / (Li + Nb) = 0.4859. Full circles: Li / (Li + Nb) = 0.5000.

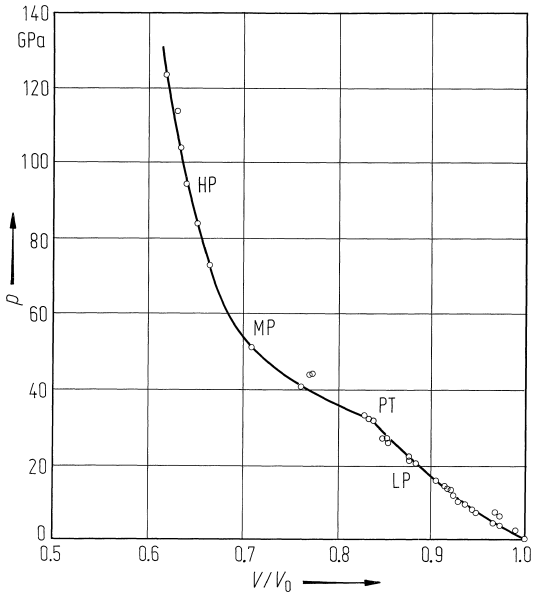

Fig. 2A-1-006. $LiNbO_3$. p vs. V/V_0 [85Got]. p: shock pressure. V/V_0: normalized volume. HP: high pressure phase, MP: mixed phase, LP: low pressure phase. PT: phase transition point.

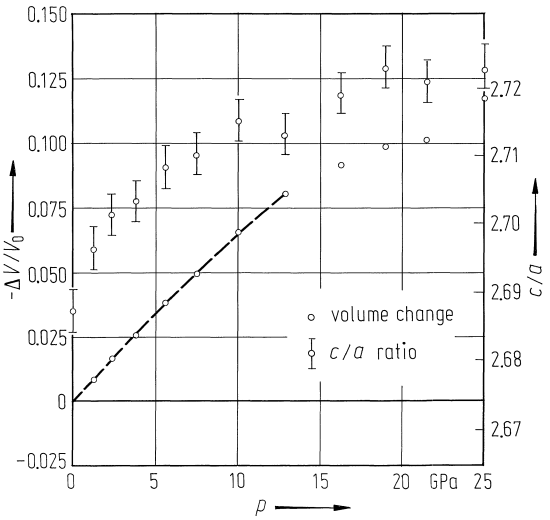

Fig. 2A-1-007. $LiNbO_3$. $-\Delta V/V_0$, c/a vs. p [85DaJ].
$-\Delta V/V_0$: volume change relative to its value at 0.15 GPa.

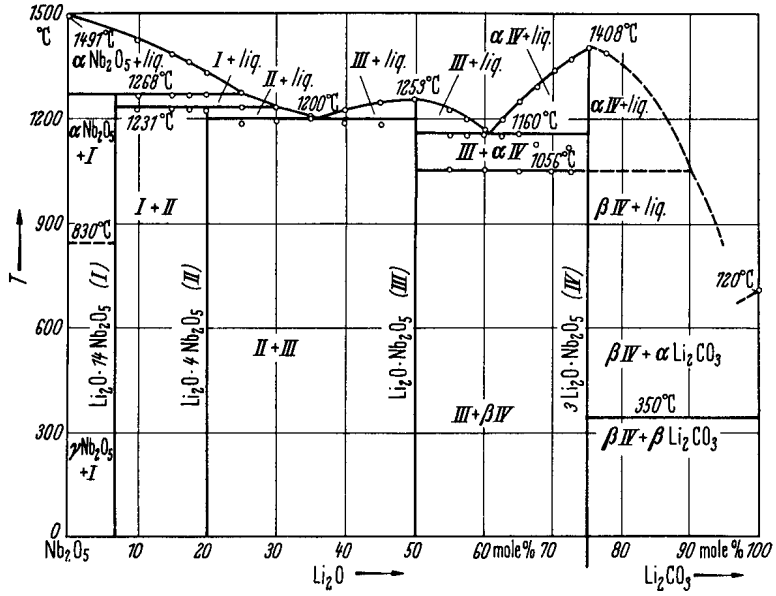

Fig. 2A-1-008. $Li_2O(Li_2CO_3)$-Nb_2O_5. Phase diagram [58Rei].

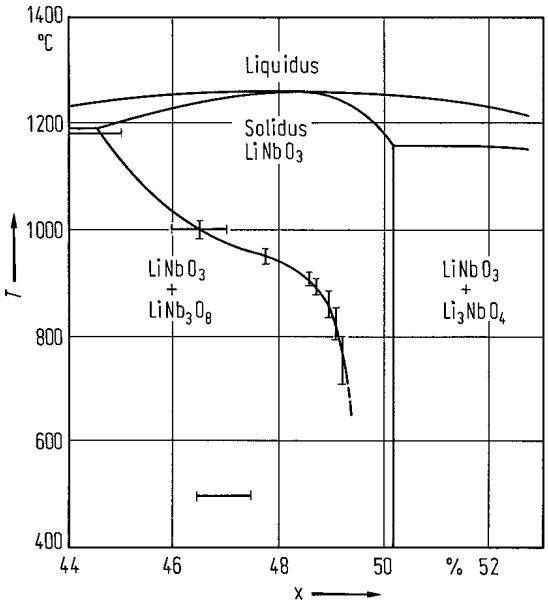

Fig. 2A-1-009. $LiNbO_3$. Phase diagram of system x $Li_2O{\cdot}(1–x)$ Nb_2O_5 [74Sva]. See also [72Sco, 68Ler].

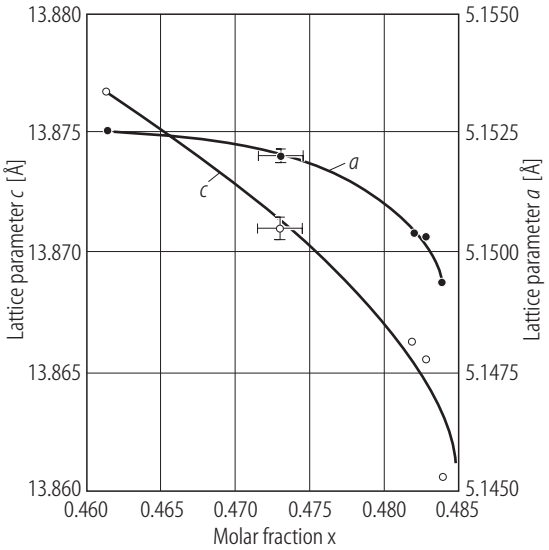

Fig. 2A-1-010. $LiNbO_3$. *a*, *c* vs. x [91Gra]. x: Li_2O content.

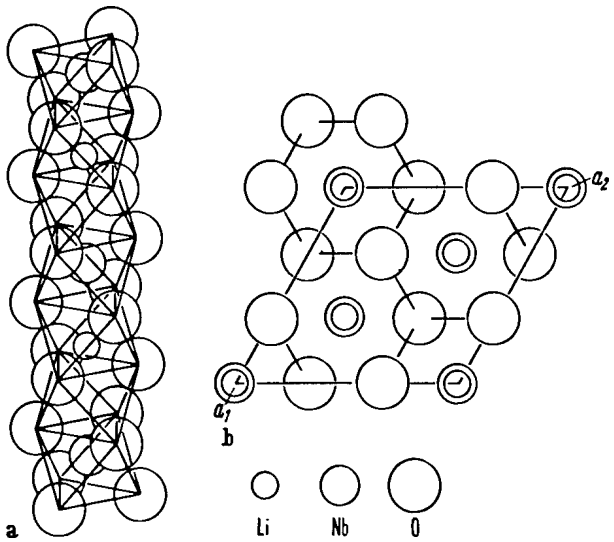

Fig. 2A-1-011. $LiNbO_3$. (**a)**: Sequences of distorted octahedra along the polar *c*-axis. (**b)**: idealized contents of one unit cell, viewed along the *c*-axis [66Abr2].

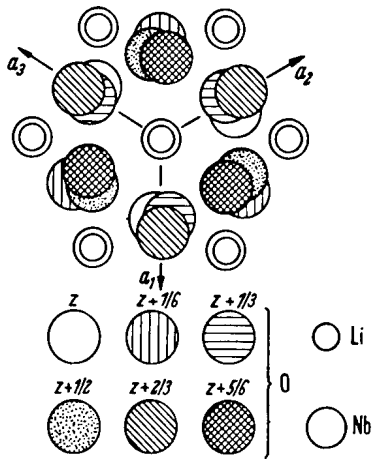

Fig. 2A-1-012. $LiNbO_3$. Arrangement of O atoms around Li and Nb atoms viewed along the *c*-axis [66Abr2].

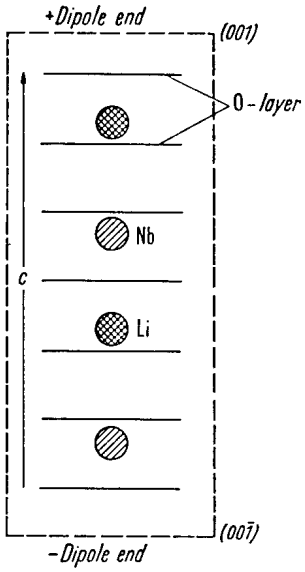

Fig. 2A-1-013. $LiNbO_3$. Oxygen layers and cations in ferroelectric phase [66Abr2]. A full period along the *c*-axis is shown. The broken line represents the outlines of a macroscopic crystal (001) and $(00\bar{1})$ being indicated.

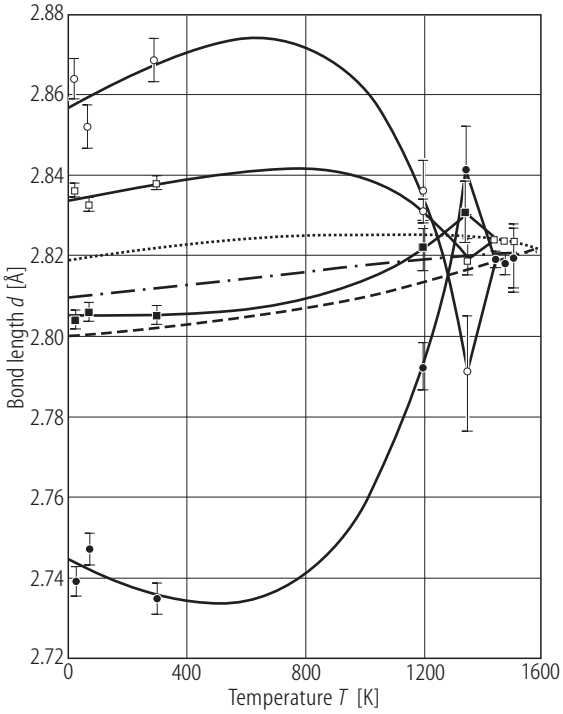

Fig. 2A-1-014. $LiNbO_3$. *d* vs. *T* [94Boy]. *d*: O–O bond length in NbO_6 octahedron: below (full circles), above (open circles), inclined 1 (full squares), inclined 2 (open squares). Dashed line: average of above and below, dotted line: average of inclined, dashed-dotted line: total average. For definitions of the bonds, see original paper.

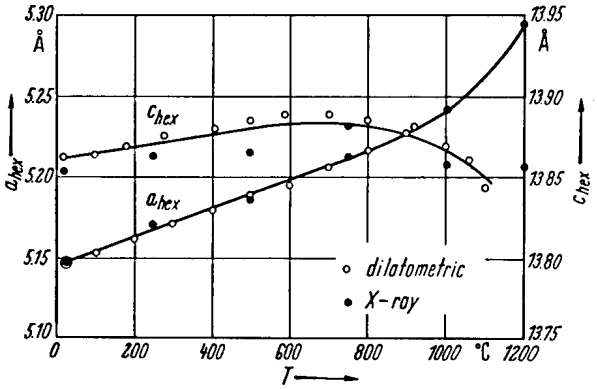

Fig. 2A-1-015. $LiNbO_3$. Lattice parameters vs. *T* [66Abr1]. See also [74Lis].

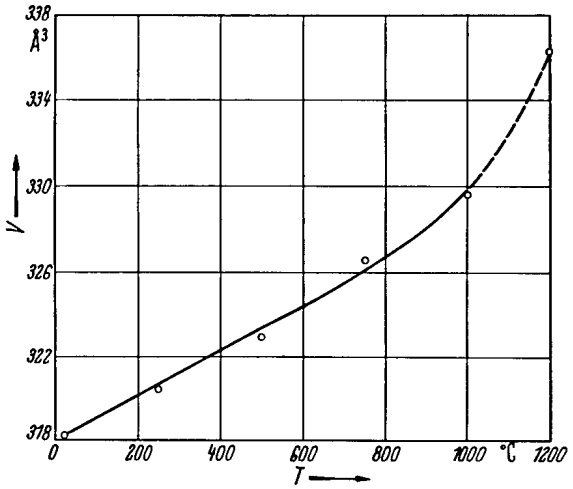

Fig. 2A-1-016. $LiNbO_3$. *V* vs. *T* [66Abr1]. *V:* volume of hexagonal unit cell.

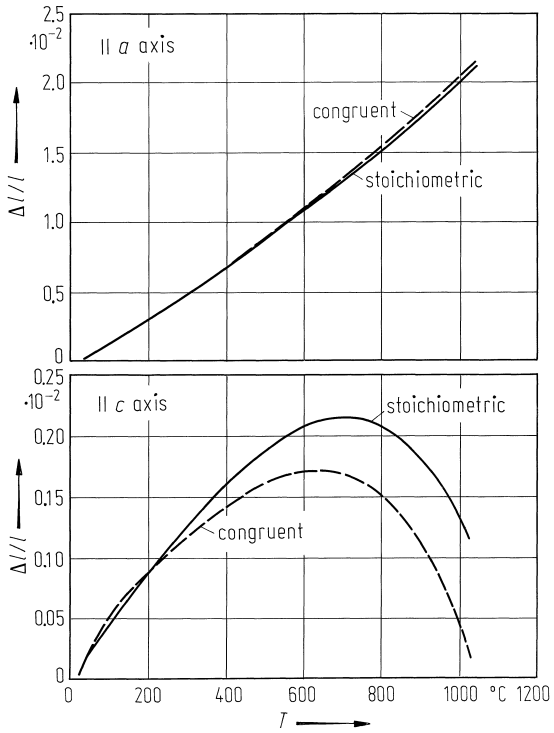

Fig. 2A-1-017. $LiNbO_3$. $\Delta l/l$ vs. T [85Gal]. $\Delta l/l$: thermal expansion. l is the length at 298 K.

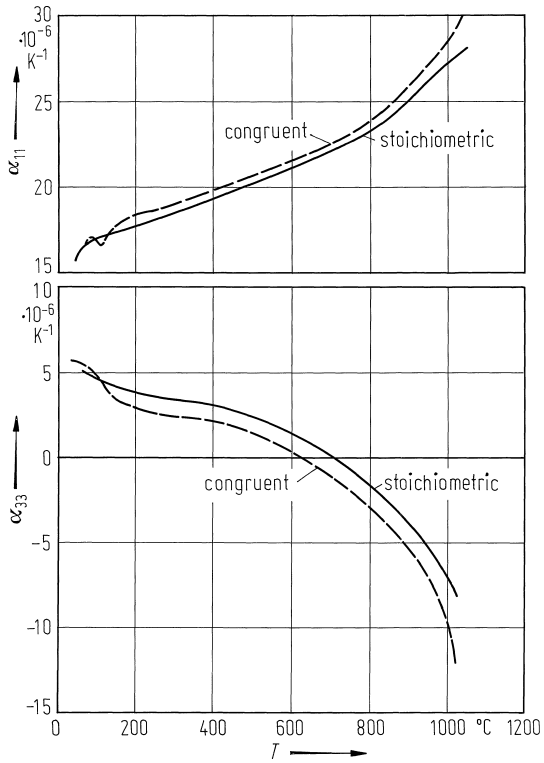

Fig. 2A-1-018. $LiNbO_3$. α_{11}, α_{33} vs. T [85Gal]. α_{ii}: thermal expansion coefficient.

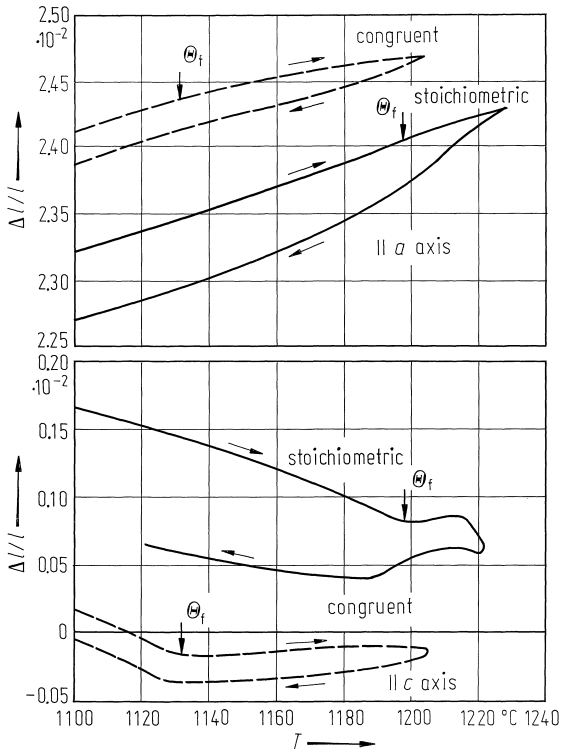

Fig. 2A-1-019. $LiNbO_3$. $\Delta l/l$ vs. T in the vicinity of Θ_f [85Gal]. $\Delta l/l$: thermal expansion. l is the length at 298 K.

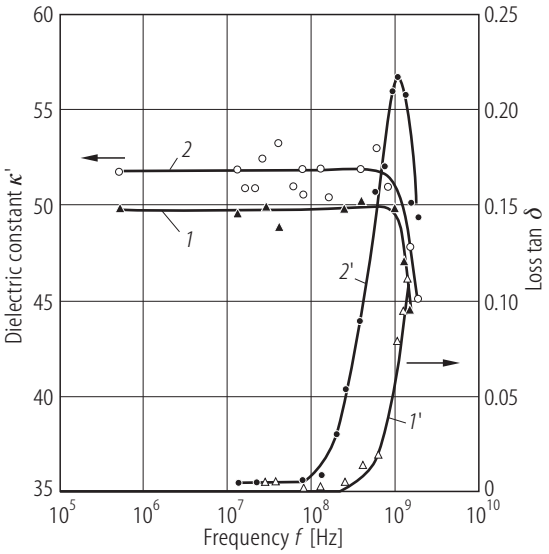

Fig. 2A-1-020. $LiNbO_3$ (ceramics). κ', $\tan\delta$ vs. f [86Rez]. T = 295 K. *1*, *1'*: unpolarized ceramics. *2*, *2'*: polarized ceramics.

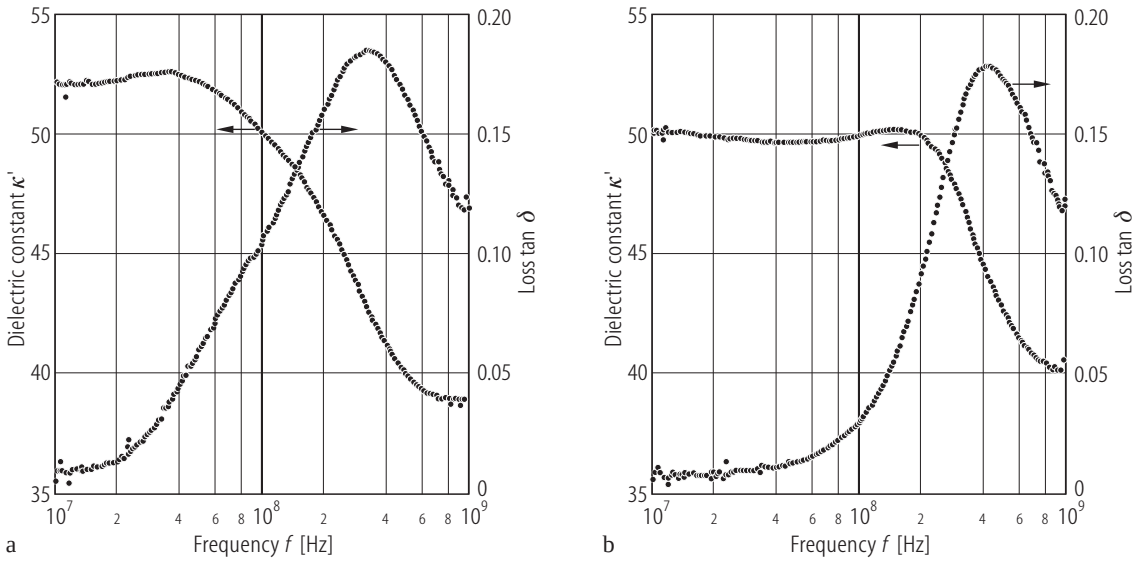

Fig. 2A-1-021. $LiNbO_3$ (ceramics). κ', $\tan\delta$ vs. $\log f$ at RT [83Yao]. (**a**) ceramics from calcined powder produced by conventional sintering. (**b**) ceramics obtained by uniaxial hot pressing.

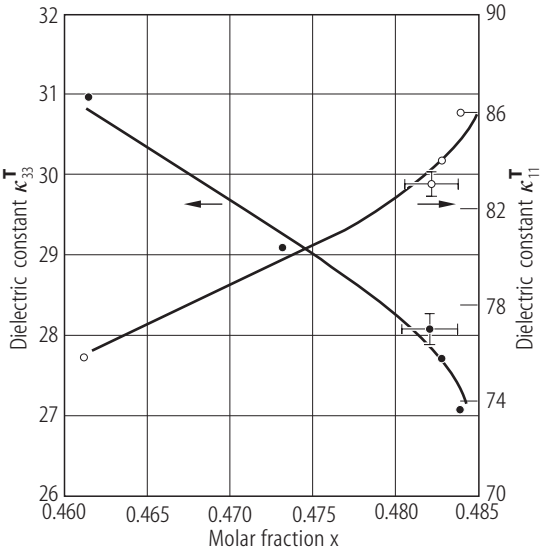

Fig. 2A-1-022. $LiNbO_3$. $\kappa_{11}^T, \kappa_{33}^T$ vs. x [91Gra]. x: Li_2O content.

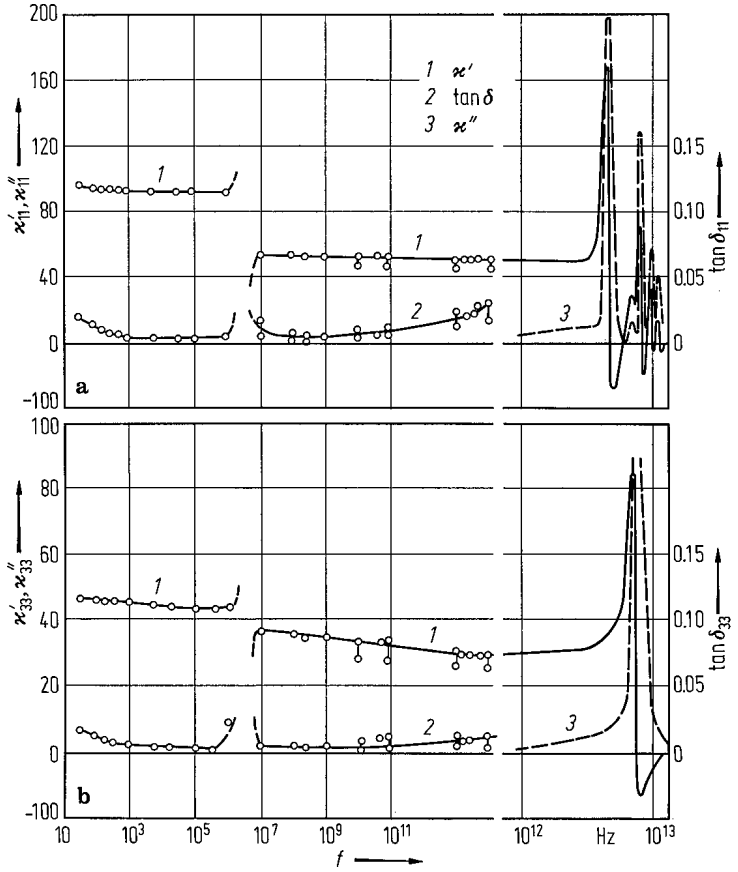

Fig. 2A-1-023. $LiNbO_3$. κ', κ'', $\tan\delta$ vs. f at 300 K [73Pop]. $\kappa''_{11\,max} = 235$, $\kappa''_{33\,max} = 155$. Note different scale above $f = 10^{12}$ Hz.

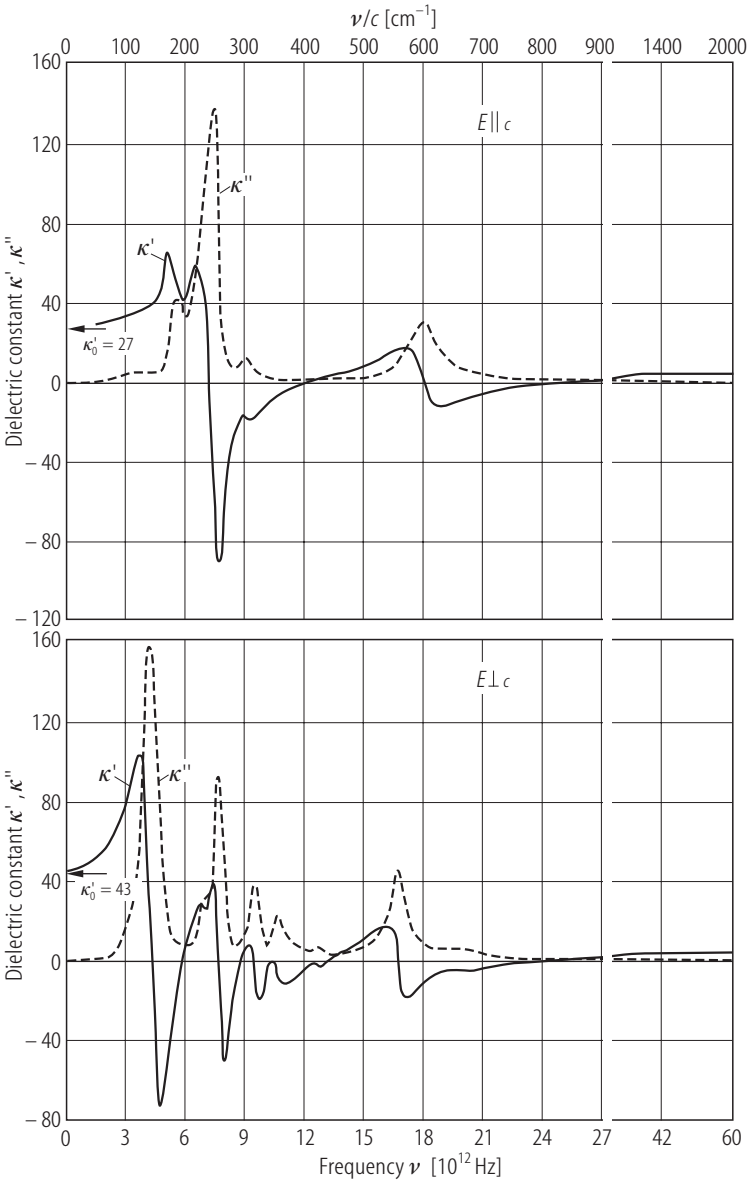

Fig. 2A-1-024. $LiNbO_3$. κ', κ'' vs. ν at RT [66Axe]. Note the change in the scale at $27 \cdot 10^{12}$ Hz.

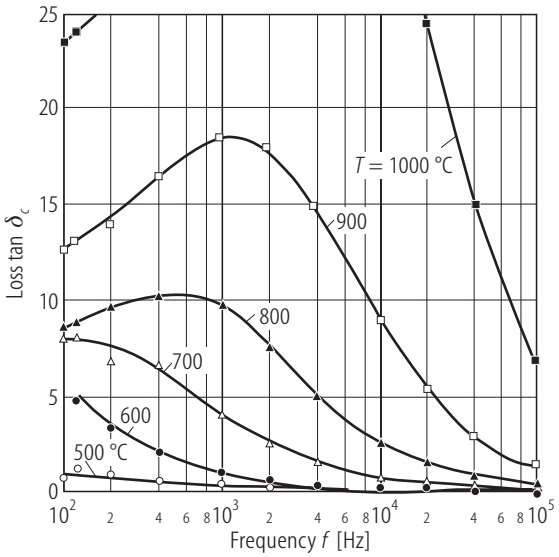

Fig. 2A-1-025. $LiNbO_3$. tanδ_c vs. f [89Ros]. Parameter: T. Crystal was grown from congruent melt (Li / Nb = 48.5/51.5).

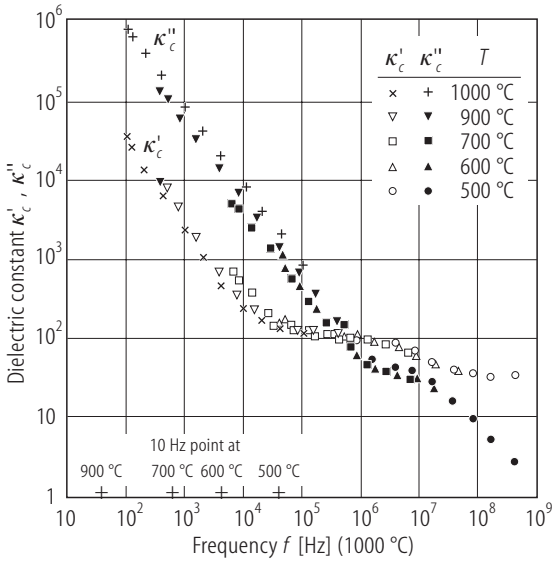

Fig. 2A-1-026. $LiNbO_3$. κ_c', κ_c'' vs. f [89Ros]. Parameter: T. The data at 900 °C, 700 °C, 600 °C and 500 °C are fitted successively to the data at 1000 °C by shifting the frequency scale. 10 Hz points at these temperatures are indicated. Crystal was grown from congruent melt (Li / Nb = 48.5/51.5).

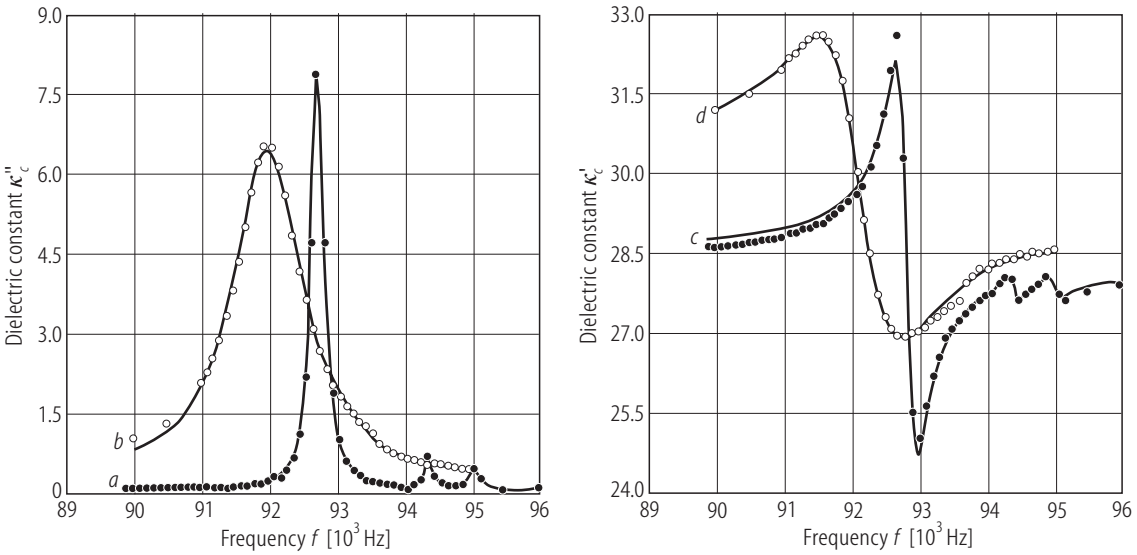

Fig. 2A-1-027. $LiNbO_3$:Fe. κ_c', κ_c'' vs. f [91Bar]. T = 294 K. 0.289 mol % Fe. *a*, *c*: before the heat treatment. *b*, *d*: after the heat treatment at 600 °C for 2 h in air.

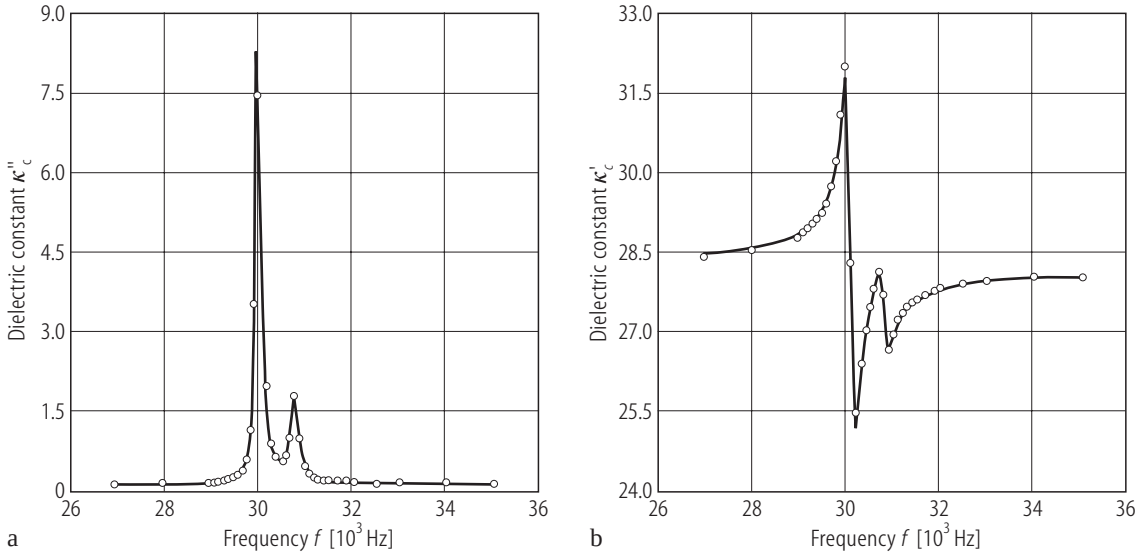

Fig. 2A-1-028. $LiNbO_3$:Fe. κ_c', κ_c'' vs. f [91Bar]. T = 294 K. 0.289 mol % Fe. a: κ_c''. b: κ_c'.

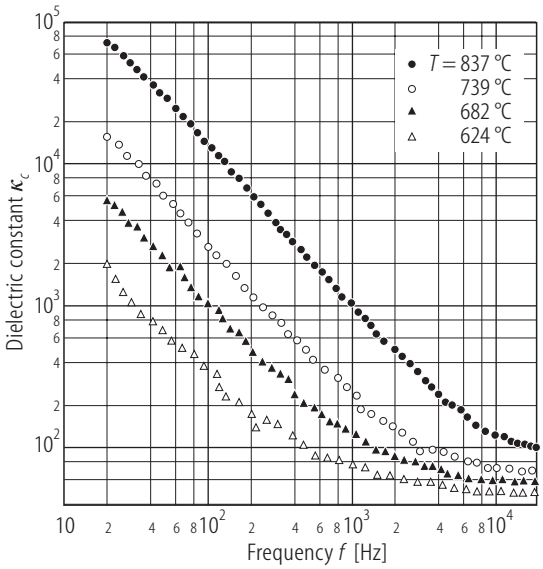

Fig. 2A-1-029. $LiNbO_3$. κ_c vs. f [85Pri]. Parameter: T.

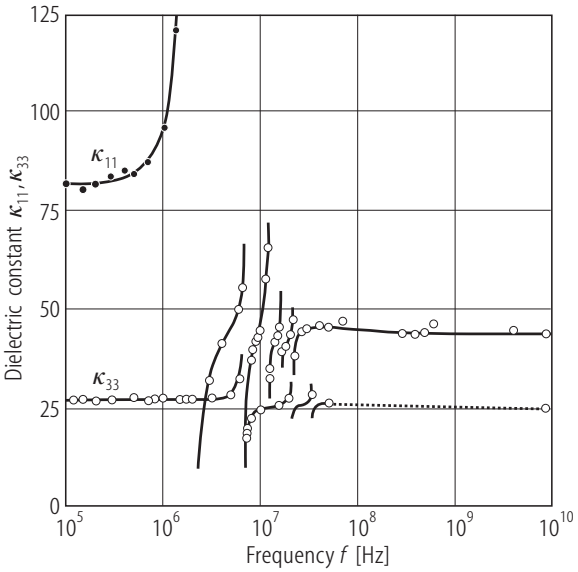

Fig. 2A-1-030. $LiNbO_3$. κ_{11}, κ_{33} vs. f [67Ohm]. T = RT.

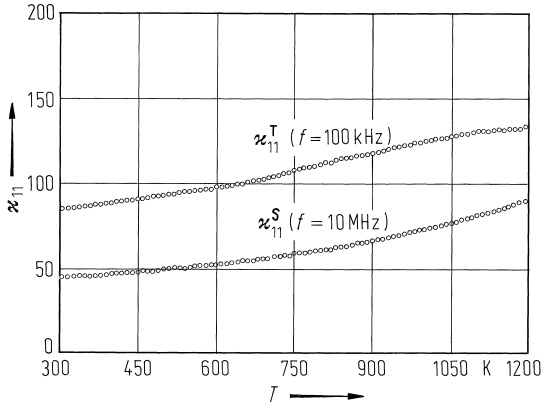

Fig. 2A-1-031. $LiNbO_3$. $\kappa_{11}^{T}, \kappa_{11}^{S}$ vs. T [87Tom]. Li / Nb = 0.942.

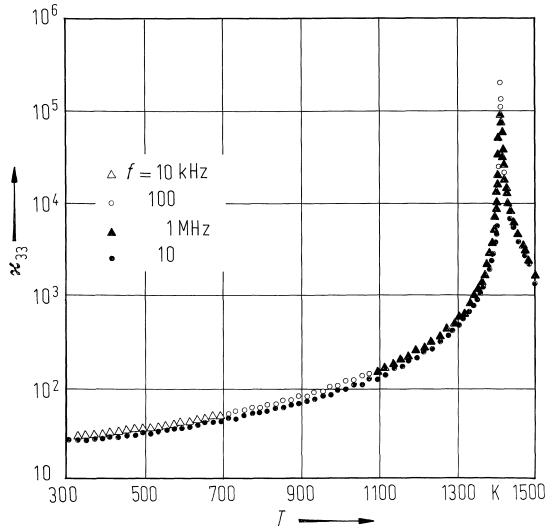

Fig. 2A-1-032. $LiNbO_3$. κ_{33} vs. T [87Tom]. Parameter: f. Li / Nb = 0.942.

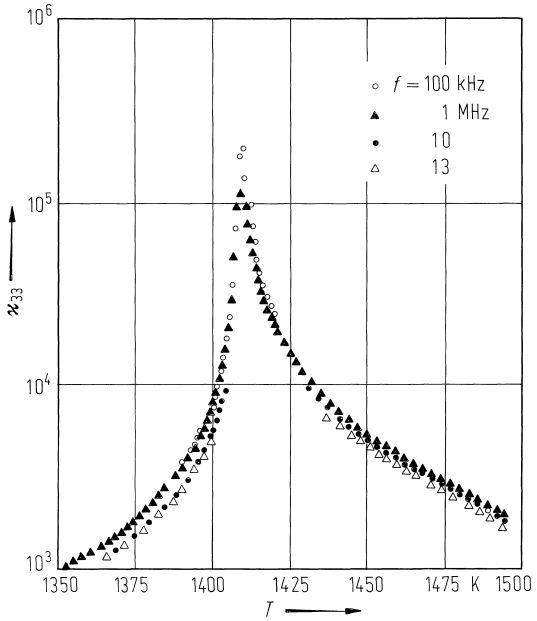

Fig. 2A-1-033. $LiNbO_3$. κ_{33} vs. T in the vicinity of Θ_f [87Tom]. Parameter: f. Li / Nb = 0.942.

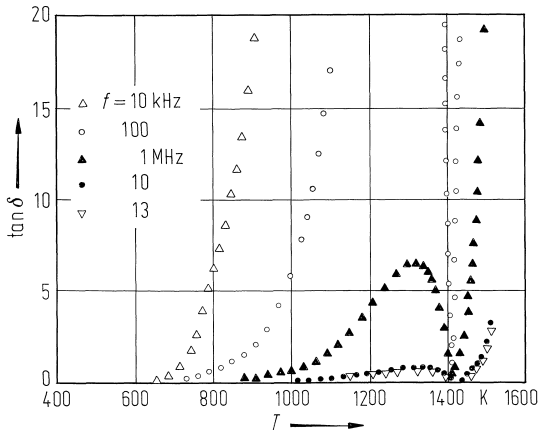

Fig. 2A-1-034. $LiNbO_3$. tanδ vs. T [87Tom]. Parameter: f.
Li / Nb = 0.942.

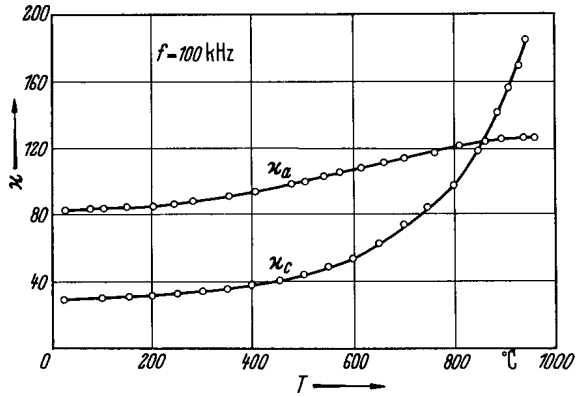

Fig. 2A-1-035. $LiNbO_3$. κ_a, κ_c vs. T [66Nas]. f = 100 kHz. See also [73Pop].

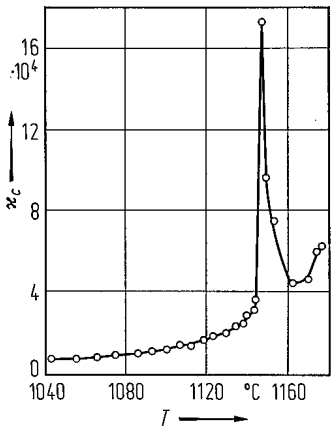

Fig. 2A-1-036. $LiNbO_3$. κ_c vs. T [68Ber]. f = 1 kHz. The crystal was pulled from a stoichiometric melt.

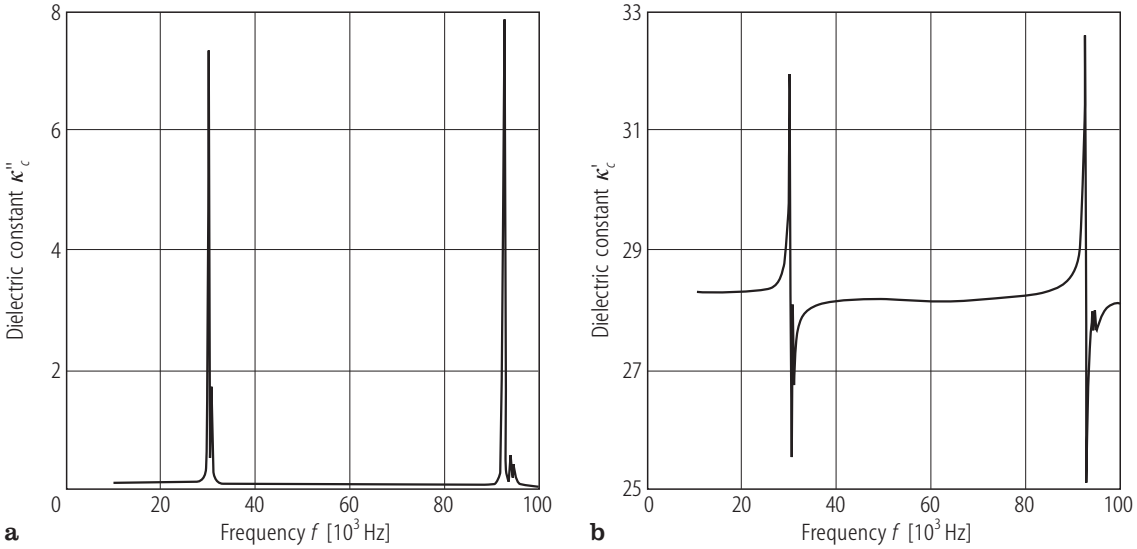

Fig. 2A-1-037. $LiNbO_3$:Fe. κ'_c, κ''_c vs. f [92Dep]. T = 294 K. Content of Fe: 0.29 mol %. a: κ''_c. b: κ'_c.

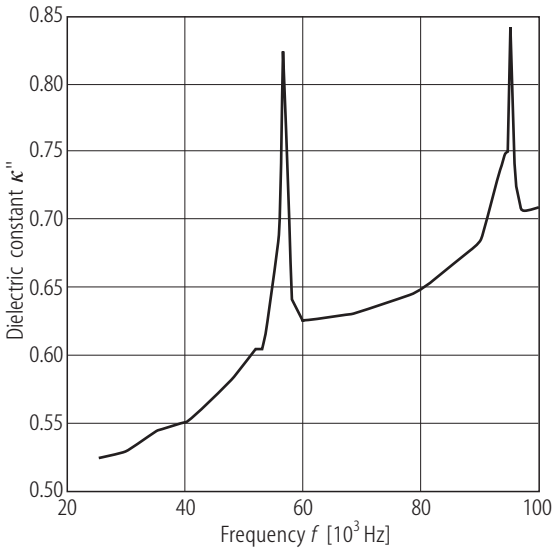

Fig. 2A-1-038. $LiNbO_3$:Fe. κ_c'' vs. f [92Dep]. T = 294 K. Content of Fe: 0.15 mol %.

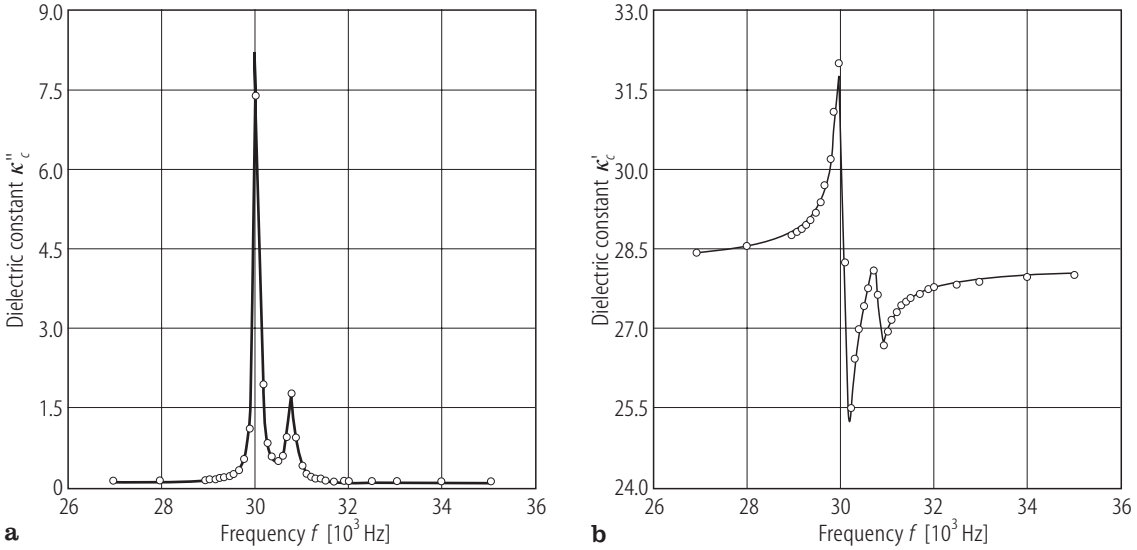

Fig. 2A-1-039. $LiNbO_3$:Fe. κ_c', κ_c'' vs. f [92Dep]. T = 294 K. Content of Fe: 0.29 mol %. Full lines are fits to the resonance formula. a: κ_c''. b: κ_c'.

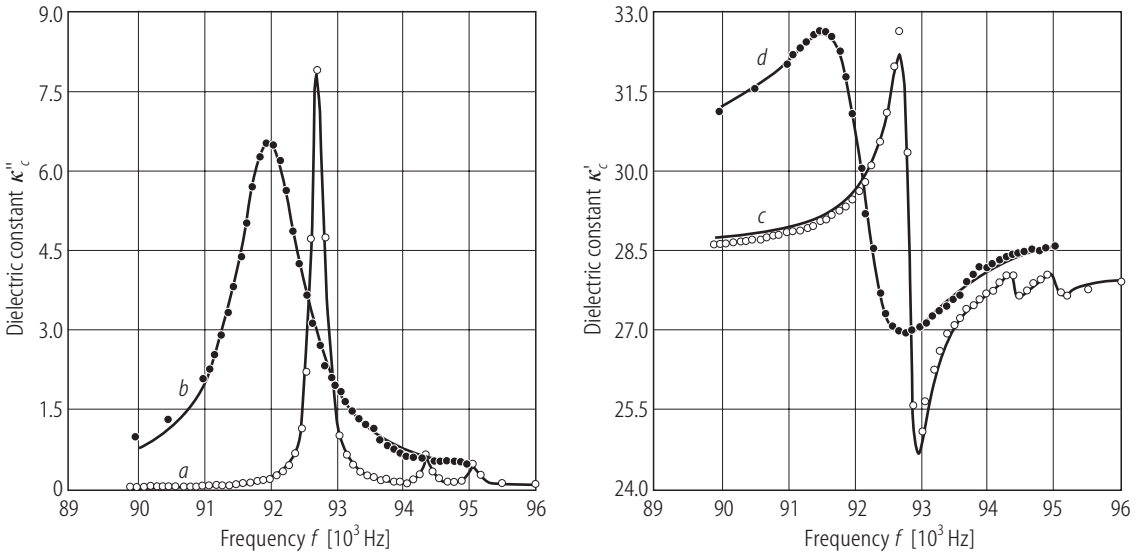

Fig. 2A-1-040. $LiNbO_3$:Fe. κ_c', κ_c'' vs. f [92Dep]. T = 294 K. Content of Fe: 0.29 mol %. Curves *a*, *c*: before heat treatment. *b*, *d*: after heating at 600 °C in air for 2 h. Full lines are fits to the resonance formula.

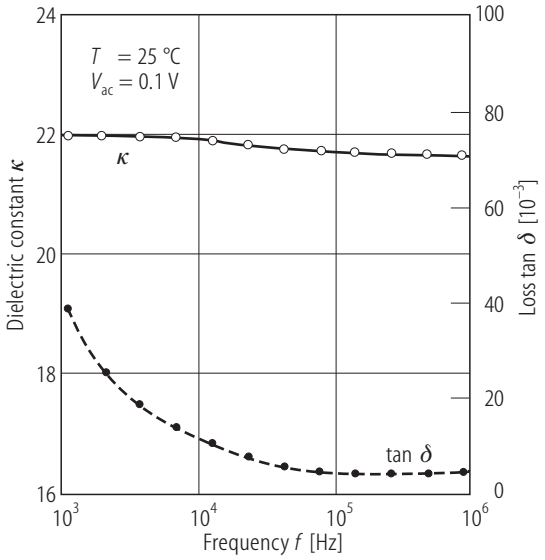

Fig. 2A-1-041. $LiNbO_3$ (thin film). κ, $\tan\delta$ vs. f [90Hag]. Sample: thin films were deposited on polycrystalline Pt by sol-gel method. d = 0.55 μm.

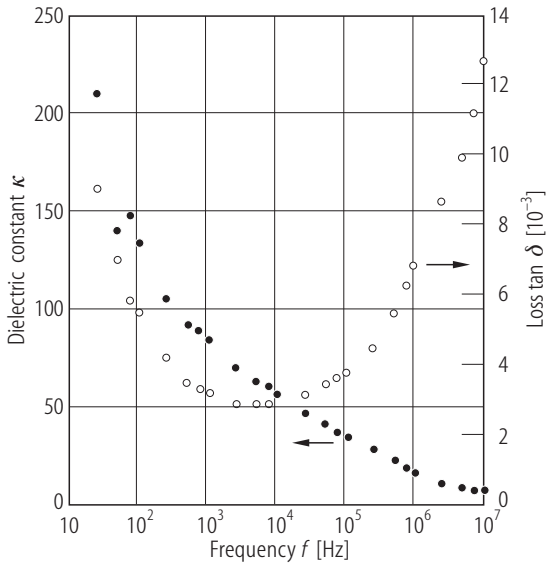

Fig. 2A-1-042. $LiNbO_3$ (thin film). κ, $\tan\delta$ vs. f [93Jos]. Thin films were deposited on (100) face of Si by a sol-gel method.

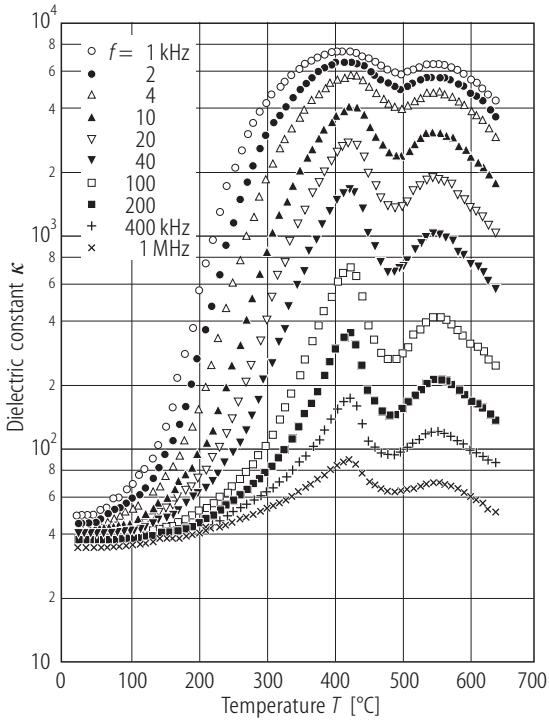

Fig. 2A-1-043. $LiNbO_3$ (amorphous thin film). κ vs. T [84Kit]. Parameter: f.

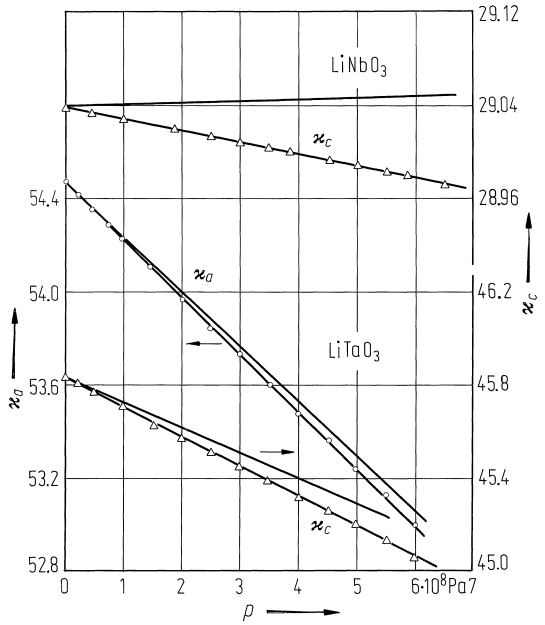

Fig. 2A-1-044. $LiNbO_3$, $LiTaO_3$. κ vs. p at 295 K [87Sam]. Solid lines represent the true pressure effects after correcting for dimensional changes. $f = 10^4$ or 10^5 Hz.

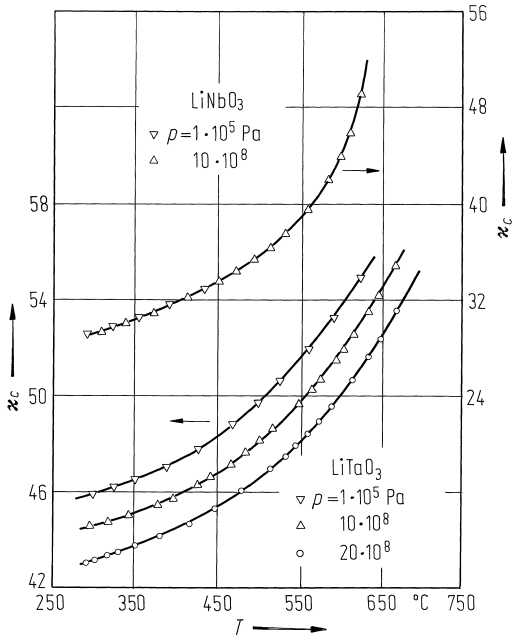

Fig. 2A-1-045. $LiNbO_3$, $LiTaO_3$. κ_c vs. T [87Sam]. Parameter: p. κ at $f = 10^4$ or 10^5 Hz.

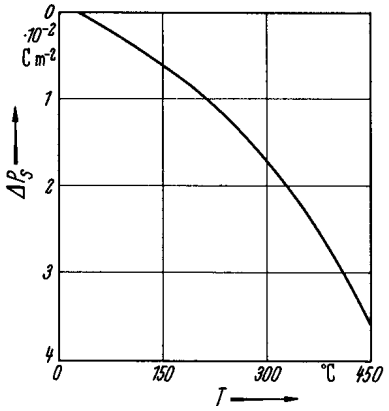

Fig. 2A-1-046. $LiNbO_3$. ΔP_s vs. T [66Sav].
$\Delta P_s = P_s(298\ K) - P_s(T)$.

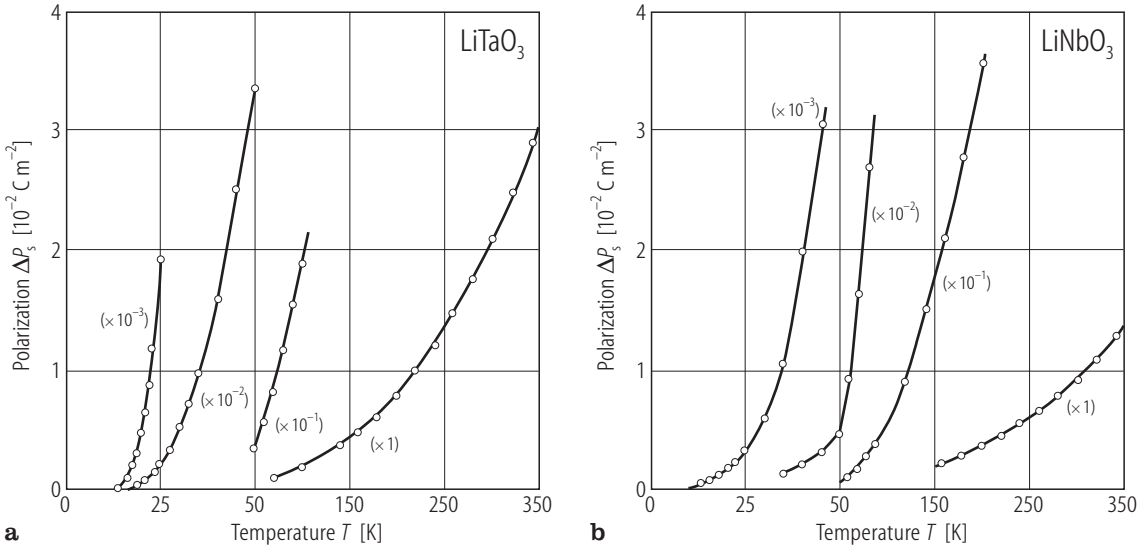

Fig. 2A-1-047. $LiNbO_3$ (**b**), $LiTaO_3$ (**a**). ΔP_s vs. T [76Gla]. $\Delta P_s = P_s(T) - P_s(0)$. Note the change of scale at 50 K.

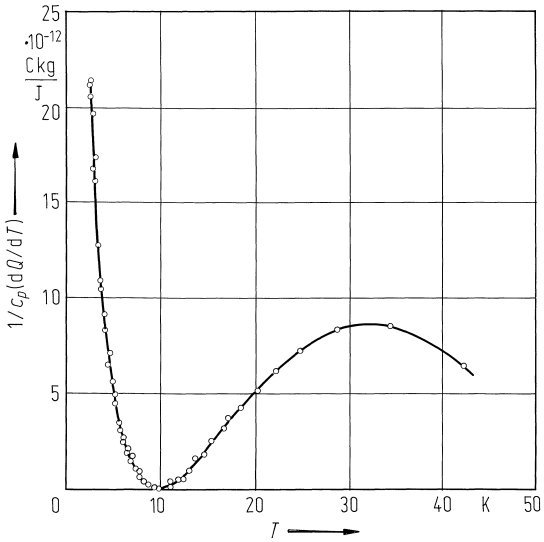

Fig. 2A-1-048. $LiNbO_3$. (dQ/dT)/c_p vs. T [81Vie]. Q: electric charge, c_p: specific heat. Sample surface area is $1.45 \cdot 10^{-4}$ m^2.

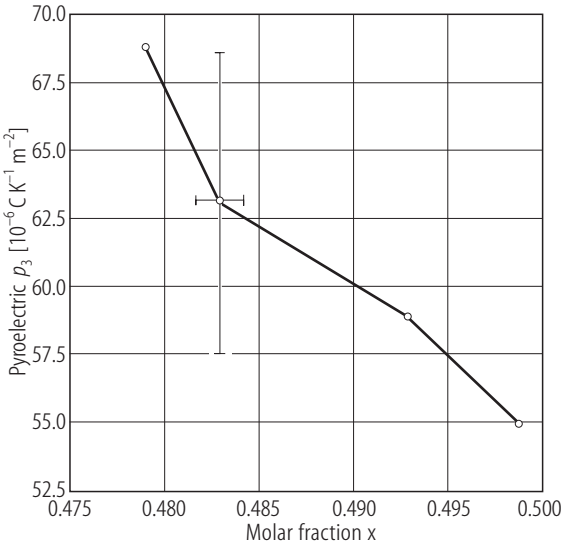

Fig. 2A-1-049. x $Li_2O·(1–x)Nb_2O_5$. p_3 vs. x [94Bar]. x: LiO_2 content in the crystal.

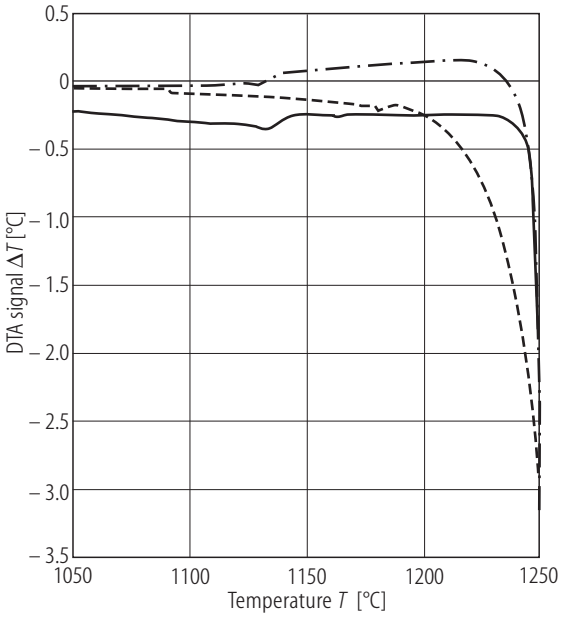

Fig. 2A-1-050. $LiNbO_3$. ΔT vs. T [88Gal]. ΔT: DTA signal. Solid line: congruent powder crystal. Dashed line: congruent crushed crystal. Dashed-dotted line: stoichiometric crushed crystal.

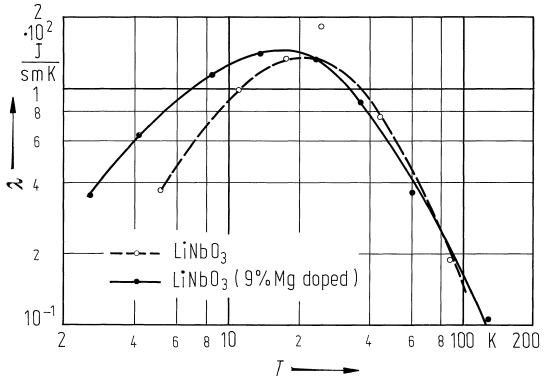

Fig. 2A-1-051. $LiNbO_3$ (undoped and Mg-doped). λ vs. T [85Bur]. λ: thermal conductivity. The composition of doped crystal is $Li_{0.901}Mg_{0.087}Nb_{0.992}O_3$.

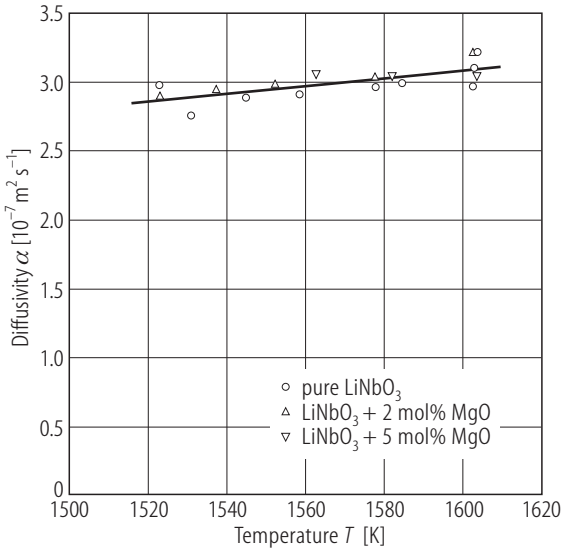

Fig. 2A-1-052. $LiNbO_3$:MgO. α vs. T [93Oga]. α: thermal diffusivity. Parameter: MgO dosage.

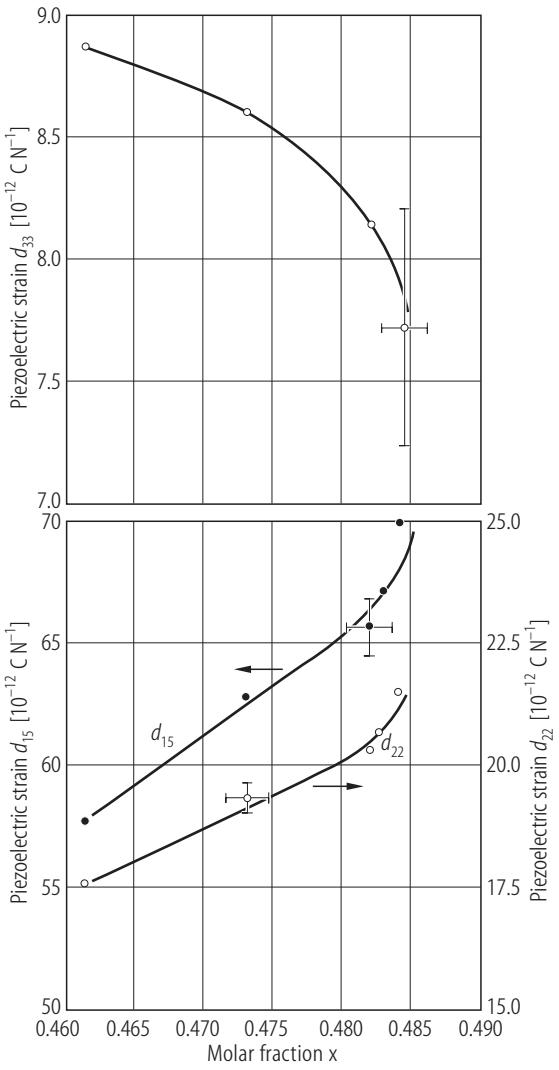

Fig. 2A-1-053. x $Li_2O{\cdot}(1–x)Nb_2O_5$. d_{15}, d_{22}, d_{33} vs. x [91Gra]. x: Li_2O content.

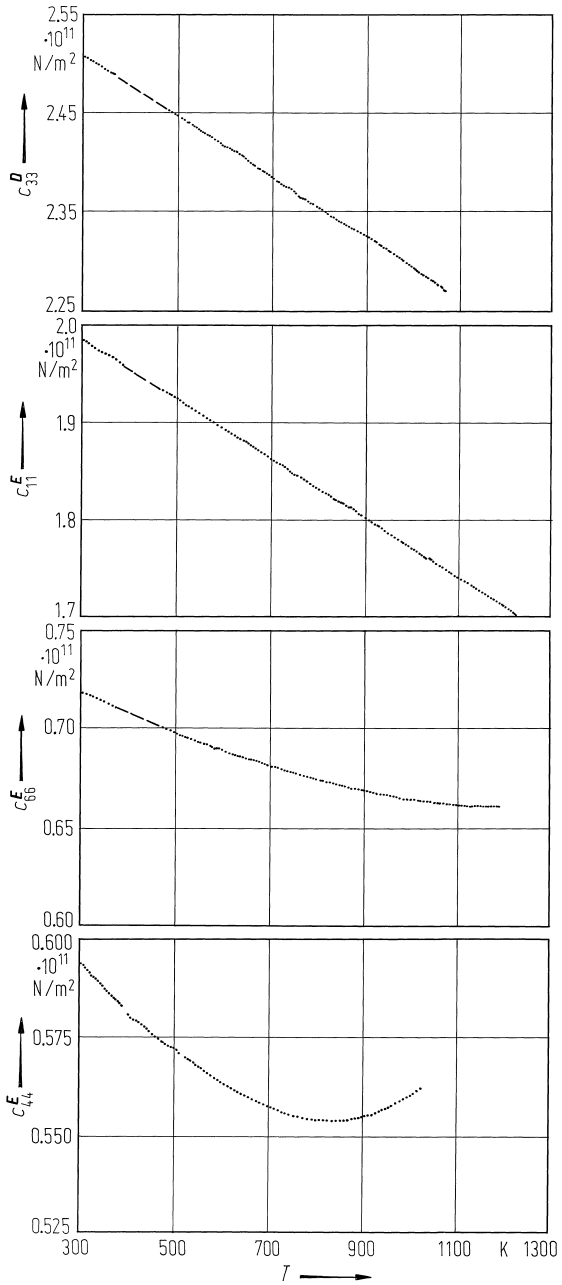

Fig. 2A-1-054. $LiNbO_3$. $c_{\lambda\mu}$ vs. T [87Tom]. $c_{\lambda\mu}$: elastic stiffness.

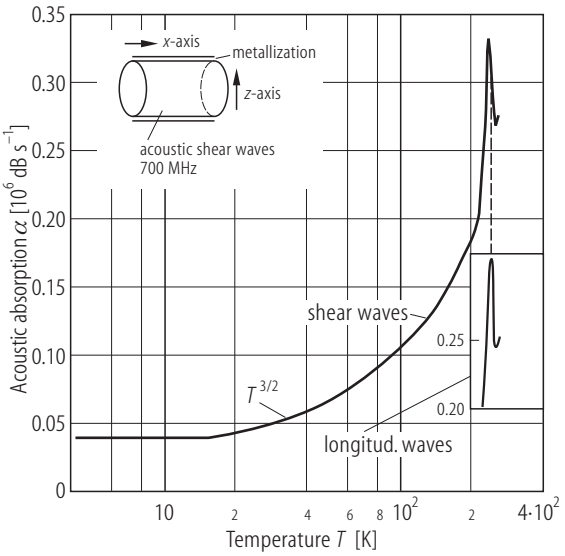

Fig. 2A-1-055. $LiNbO_3$. α vs. T [89LiJ]. α: attenuation coefficient of the ultrasonic shear wave at 700 MHz propagating along the *x* axis.

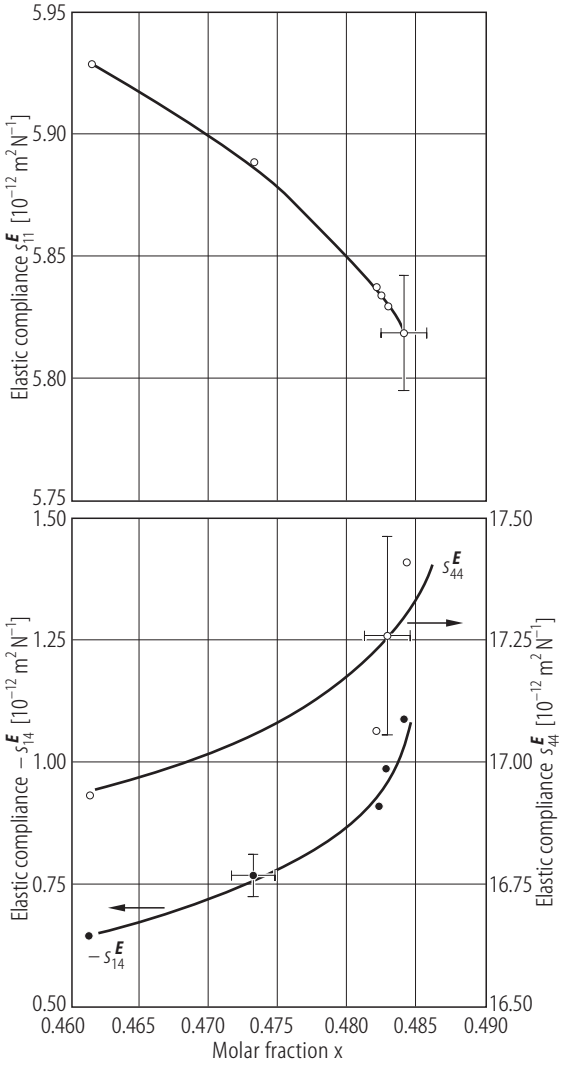

Fig. 2A-1-056. $LiNbO_3$. s_{11}^E, $-s_{14}^E$, s_{44}^E vs. x [91Gra]. x: Li_2O content.

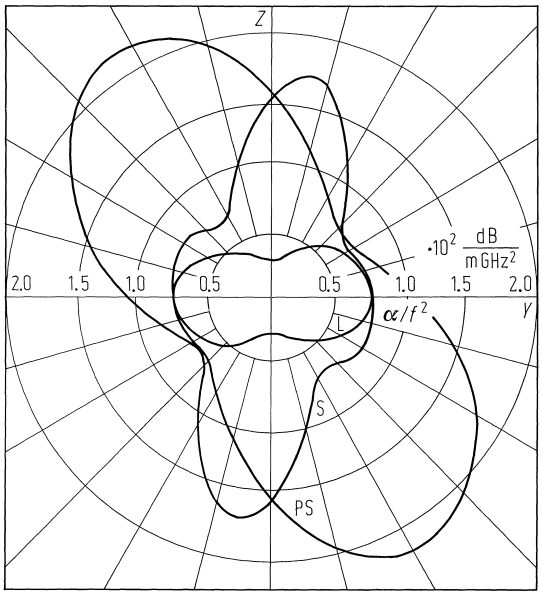

Fig. 2A-1-057. $LiNbO_3$. Anisotropy of α/f^2 in *YZ* plane [81Baj]. α: attenuation constant, *f*: frequency in GHz, α/f^2: attenuation constant normalized to 1 GHz. L: longitudinal wave, S: shear wave, PS: pure shear wave.

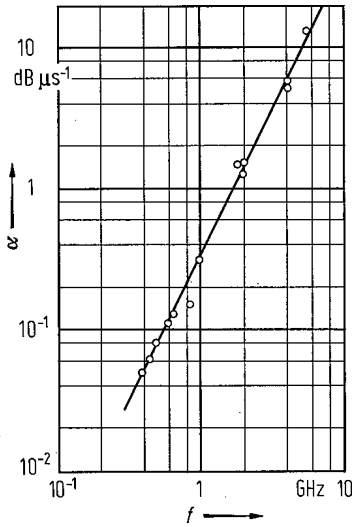

Fig. 2A-1-058. $LiNbO_3$. α vs. f [66Wen]. α: acoustic longitudinal wave attenuation along the *c*-axis at RT.

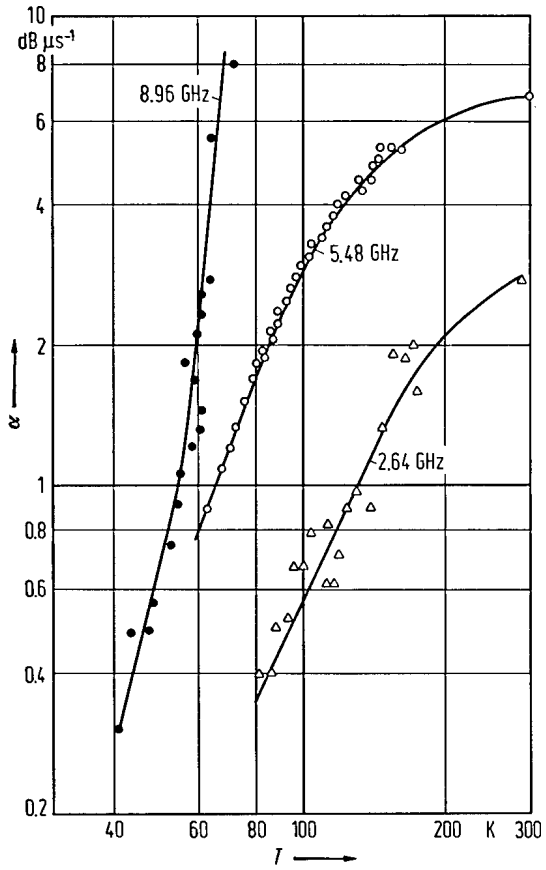

Fig. 2A-1-059. $LiNbO_3$. α vs. T [66Gra]. Parameter: f. α: acoustic longitudinal wave attenuation along the c-axis.

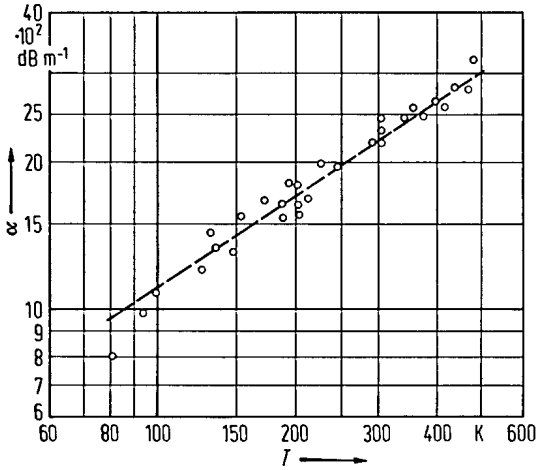

Fig. 2A-1-060. $LiNbO_3$. α vs. T [69Far]. α: acoustic longitudinal wave attenuation along the *c*-axis at 8.9 GHz. The broken line shows the relation $\alpha = 53\ T^{0.66}$ dB m^{-1}.

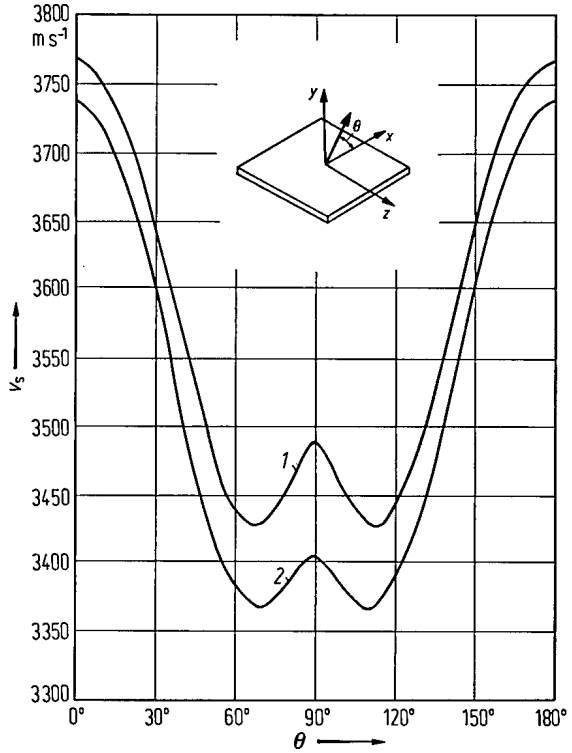

Fig. 2A-1-061. $LiNbO_3$. v_s vs. θ [68Cam]. v_s: acoustic surface wave velocity in the *y*-cut plane, θ: angle between the direction of wave propagation and the *x*-axis. Curve *1*: ordinary surface wave propagation, curve *2*: surface wave propagation with perfect conduction at the crystal surface.

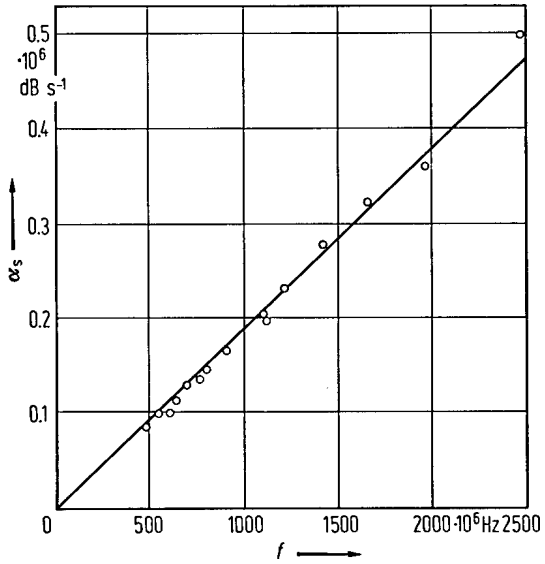

Fig. 2A-1-062. $LiNbO_3$. α_s vs. f [76Slo]. α_s: acoustic surface wave attention due to air loading for y-cut, z-propagating.

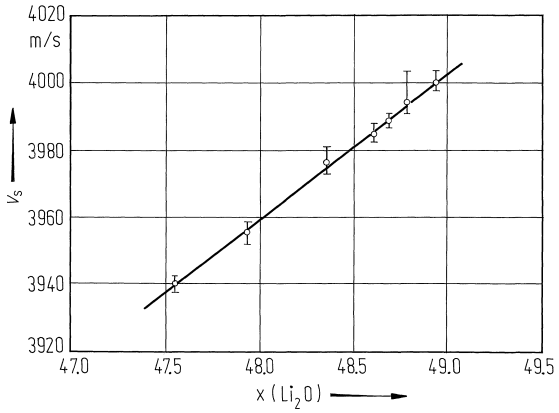

Fig. 2A-1-063. $LiNbO_3$. v_s vs. x [87Yam]. v_s: surface acoustic velocity propagating along the *X*-axis on the free surface of 128° rotated *Y*-cut plate, x: Li_2O mol % in $LiNbO_3$.

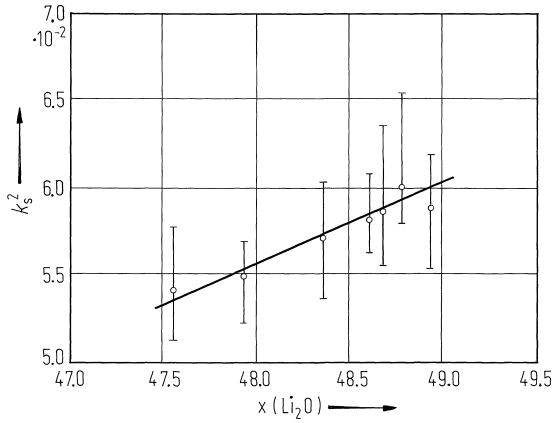

Fig. 2A-1-064. $LiNbO_3$. k_s^2 vs. x [87Yam]. k_s^2: surface acoustic coupling constant propagating along the *X*-axis on 128° rotated *Y*-cut plate, x: Li_2O mol % in $LiNbO_3$.

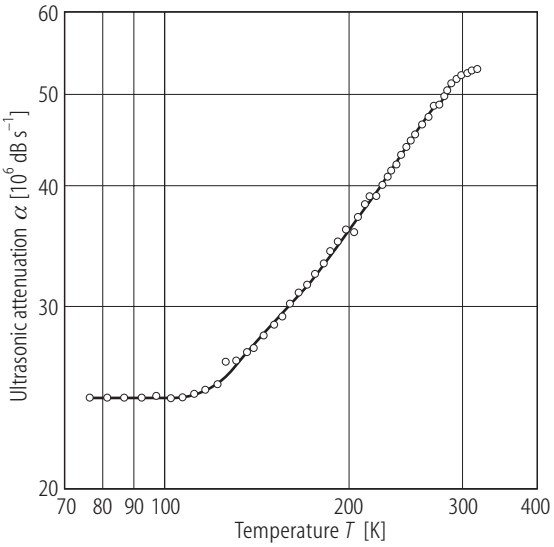

Fig. 2A-1-065. $LiNbO_3$. α vs. T [87Baz]. α: ultrasonic attenuation. f = 9.1 GHz. Longitudinal wave propagating along the x-axis.

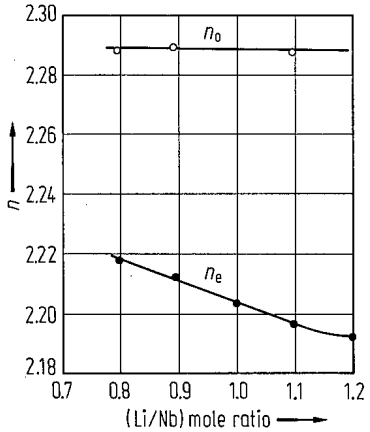

Fig. 2A-1-066. $LiNbO_3$. *n* vs. melt composition [68Ber].
λ = 632.8 nm.

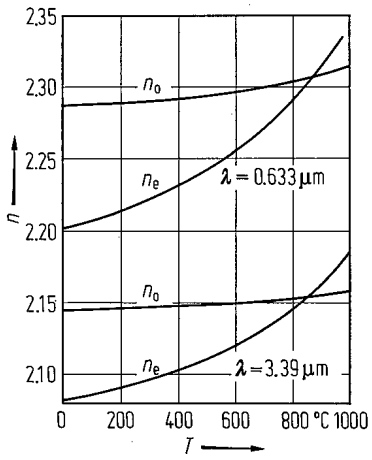

Fig. 2A-1-067. $LiNbO_3$. n vs. T [76Smi]. The crystal was grown from a congruent melt. See also [68Iwa].

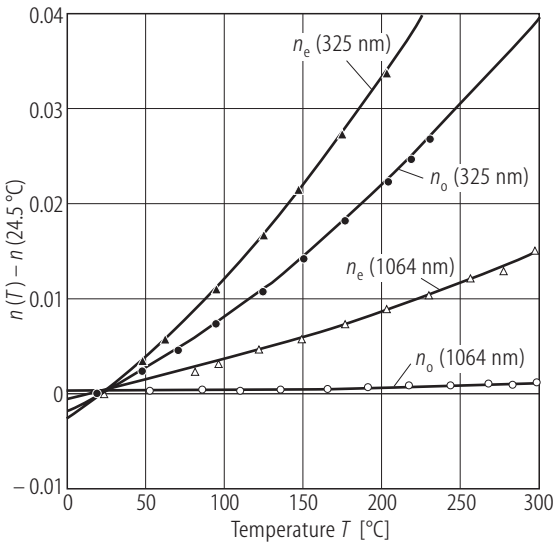

Fig. 2A-1-068. $LiNbO_3$. $n_o - n_o$ (24.5 °C), $n_e - n_e$ (24.5 °C) vs. T [90Jun]. Parameter: λ. Sample: almost stoichiometric (Li/Nb $\cong$ 1.00) crystal prepared by vapor transport equilibrium (VTE).

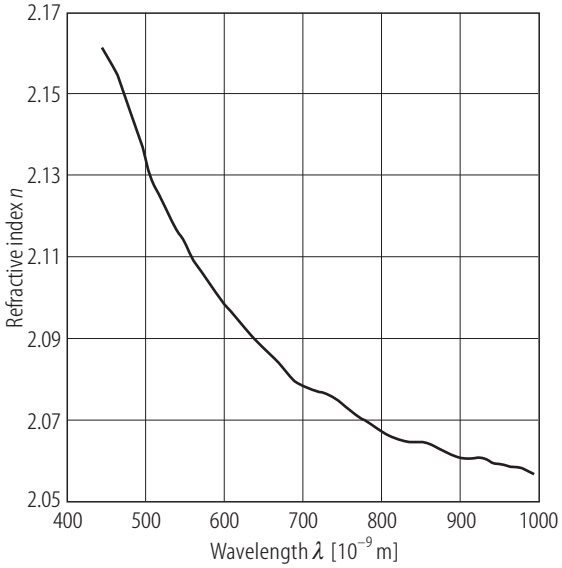

Fig. 2A-1-069. $LiNbO_3$ (thin film). n vs. λ [92Ben]. Sample: thin film prepared by RF sputtering.